Review of Scientific Instruments

Generating circularly polarized radiation in the extreme ultraviolet spectral range at the free-electron laser FLASH

Cite as: Rev. Sci. Instrum. **88**, 053903 (2017); https://doi.org/10.1063/1.4983056
Submitted: 09 March 2017 . Accepted: 19 April 2017 . Published Online: 17 May 2017

Clemens von Korff Schmising, David Weder, Tino Noll, Bastian Pfau, Martin Hennecke, Christian Strüber, Ilie Radu, Michael Schneider, Steffen Staeck, Christian M. Günther, Jan Lüning, Alaa el dine Merhe, Jens Buck, Gregor Hartmann, Jens Viefhaus, Rolf Treusch, and Stefan Eisebitt

REVIEW OF SCIENTIFIC INSTRUMENTS **88**, 053903 (2017)

Generating circularly polarized radiation in the extreme ultraviolet spectral range at the free-electron laser FLASH

Clemens von Korff Schmising,[1] David Weder,[1] Tino Noll,[1] Bastian Pfau,[1] Martin Hennecke,[1] Christian Strüber,[1] Ilie Radu,[1] Michael Schneider,[1] Steffen Staeck,[2] Christian M. Günther,[2] Jan Lüning,[3,4] Alaa el dine Merhe,[3,4] Jens Buck,[5] Gregor Hartmann,[5,6] Jens Viefhaus,[5] Rolf Treusch,[5] and Stefan Eisebitt[1,2]

[1]*Max-Born-Institut Berlin, Max-Born-Str. 2a, 12489 Berlin, Germany*
[2]*Institut für Optik und Atomare Physik, Technische Universität Berlin, 10623 Berlin, Germany*
[3]*Sorbonne Universités, UPMC Université Paris 06, UMR 7614, LCPMR, 75005 Paris, France*
[4]*CNRS, UMR 7614, LCPMR, 75005 Paris, France*
[5]*Deutsches Elektronen-Synchrotron DESY, 22607 Hamburg, Germany*
[6]*Institut für Physik und CINSaT, Universität Kassel, Heinrich-Plett-Straße 40, 34132 Kassel, Germany*

(Received 9 March 2017; accepted 19 April 2017; published online 17 May 2017)

A new device for polarization control at the free electron laser facility FLASH1 at DESY has been commissioned for user operation. The polarizer is based on phase retardation upon reflection off metallic mirrors. Its performance is characterized in three independent measurements and confirms the theoretical predictions of efficient and broadband generation of circularly polarized radiation in the extreme ultraviolet spectral range from 35 eV to 90 eV. The degree of circular polarization reaches up to 90% while maintaining high total transmission values exceeding 30%. The simple design of the device allows straightforward alignment for user operation and rapid switching between left and right circularly polarized radiation. [http://dx.doi.org/10.1063/1.4983056]

I. INTRODUCTION

Circularly polarized radiation in the extreme ultraviolet (XUV) spectral range is a powerful tool for element specific investigations of chirality-sensitive light-matter interaction, for example, in molecules with handedness[1] or in magnetic materials. In particular, magnetic circular dichroism spectroscopy is a unique technique for transient absorption and reflection spectroscopy,[2] time resolved magnetic small-angle scattering,[3] and coherent imaging experiments[4] combining element selective magnetic sensitivity with nanometer spatial resolution.

While polarization control of electromagnetic radiation in the optical wavelength range is well established and can be very accurately adjusted with birefringent crystals or sheet polarizers in transmission geometry, the very short attenuation length in the extreme ultraviolet spectral range requires a different approach based on reflection. It is well known that for absorbing materials with a complex index of refraction, a characteristic phase shift occurs upon reflection, i.e., incident linearly polarized light with non-zero *s*- and *p*-components will in general become elliptically polarized after reflection off a metallic surface.[5] Very early reflection-based devices have been successfully used for polarization studies in the XUV spectral range[6–9] and to generate and analyze circularly polarized light at synchrotron facilities[10–14] with applications in magnetic circular dichroism experiments of ferromagnetic Fe, Co, and Ni.[15,16] With the increasing availability and performance of laser driven high harmonic sources operating in the XUV spectral range, reflection-based polarizers have been rediscovered[17] and applied for ultrafast multi-color magnetic absorption spectroscopy.[2] In this context, it is worthwhile to mention that circularly polarized XUV radiation can also be generated directly via bi-circular driving fields in high harmonic generation. While this was already theoretically predicted[18] and experimentally demonstrated[19] more than 20 years ago, the maturity of laser and high harmonic technology has led to a renaissance of this technique with several very promising experimental implementations in the last few years.[20–22] Also, it was recently demonstrated that the polarization from an initially unpolarized lab based XUV plasma source can be efficiently controlled with a reflection based apparatus and used for magnetic circular dichroism measurements.[23] Finally, elliptically polarized light may also be generated by transmission through magnetic foils due to resonant magnetic circular dichroism,[24–26] however, inherently limited to the bandwidth of the core hole transition and only with moderate performance.

While undulators, which allow to adjust the positions of their magnet arrays for full control of the polarization, have been successfully commissioned at the new free electron laser (FEL) facility FERMI at Elettra (Trieste)[27] and LCLS at SLAC (Stanford)[28] as well as being planned for future facilities at SwissFEL and the European XFEL, the very first XUV FEL FLASH1 at DESY—in user operation since 2005—started with a fixed-gap undulator and does hence so far solely deliver linearly polarized light pulses. On the other side, at FLASH2 which started user operation in April 2016, variable gap undulators are employed and an

additional short undulator with tunable polarization will be integrated soon. Replacing the undulators at FLASH1 for variable-gap undulators including polarization control is presently envisaged for ~2020. Therefore, a mirror based polarizer is an excellent intermediate step to gain control over the polarization.

In this contribution, we present a four-mirror reflection polarizer which was recently commissioned at FLASH1. After a brief theoretical description of polarization based on the Stokes formalism and details on calculations describing the phase control via reflection, we elaborate on the main design features of the four-mirror polarizer. The performance of the device is then demonstrated in three independent measurements. First, a polarimeter measurement at a synchrotron facility shows good agreement with the predicted broadband performance with degrees of polarization reaching up to 90% while maintaining a high reflectivity of few ten percent. Second, a multichannel electron time-of-flight measurement at 60 eV confirms the high degree of circular polarization of 85%. Finally a coherent imaging experiment of nanoscale magnetic domains via circular magnetic dichroism unambiguously proves the high degree of circularly polarized light and highlights the simple and robust design of the device for user operation.

II. THEORETICAL DESCRIPTION OF POLARIZATION BASED ON THE STOKES FORMALISM

Electromagnetic radiation in free space is described as a two-dimensional transverse wave with its electric field vector $\boldsymbol{E}$ oscillating perpendicular to the propagation vector $\boldsymbol{k}$. $\boldsymbol{E}$ can be decomposed into two orthogonal components, E_p and E_s, parallel and perpendicular to the plane of incidence of the four-mirror reflection polarizer, respectively (compare Figure 2(a))

$$\boldsymbol{E}(z,t) = \begin{pmatrix} E_p e^{i\tilde{\Delta}} \\ E_s \end{pmatrix} e^{-i(\omega t - kz)}. \tag{1}$$

The oscillation frequency ω defines the time interval $2\pi/\omega$ of one revolution of the electric field vector, which amounts to the very short time of only 70 attoseconds for XUV pulses with a wavelength of $\lambda = 20\,\mathrm{nm}$. The magnitude of the angular wave vector is given by $k = 2\pi/\lambda$ and $\tilde{\Delta}$ is the relative phase of the oscillations along the p and s direction. In the special case of linear polarization $\tilde{\Delta} = 0\,or\,\pi$, for perfectly right/left circular polarization $\tilde{\Delta} = \pm\pi/2$ and $E_p = E_s$.

The state of polarization is fully defined by the four-dimensional Stokes vector S,[5]

$$S = \begin{pmatrix} S_0 \\ S_1 \\ S_2 \\ S_3 \end{pmatrix} = \begin{pmatrix} \langle E_p E_p^* \rangle + \langle E_s E_s^* \rangle \\ \langle E_p E_p^* \rangle - \langle E_s E_s^* \rangle \\ \langle E_p E_s^* \rangle + \langle E_s E_p^* \rangle \\ \langle iE_p E_s^* \rangle - \langle iE_s E_p^* \rangle \end{pmatrix}, \tag{2}$$

where the average bracket represents a time average. For perfectly polarized light, the Stokes parameters satisfy the identity

$$S_0^2 = S_1^2 + S_2^2 + S_3^2. \tag{3}$$

Assuming an angle α between the linearly polarized FLASH1 pulses and the circular polarizer as shown in Fig. 2(c), the normalized Stokes vector S_Pol in the sp-coordinate system is calculated according to

$$S_\mathrm{Pol} = R(\alpha) S_\mathrm{lin}/I_0 = \begin{pmatrix} 1 \\ \cos(2\alpha) \\ -\sin(2\alpha) \\ 0 \end{pmatrix}, \tag{4}$$

where I_0 is the intensity of the incident radiation and $R(\alpha)$ denotes the rotation matrix around propagation wave vector $\boldsymbol{k}$,[29]

$$R(\alpha) = \begin{pmatrix} 1 & 0 & 0 & 0 \\ 0 & \cos(2\alpha) & \sin(2\alpha) & 0 \\ 0 & -\sin(2\alpha) & \cos(2\alpha) & 0 \\ 0 & 0 & 0 & 1 \end{pmatrix}. \tag{5}$$

Linear p $-$ ($\alpha = 90°$) and s $-$ ($\alpha = 0°$) polarized light is $S_\mathrm{lin}/\mathrm{I}_0 = (1\ \pm 1\ 0\ 0)'$. Right and left circularly polarized light is accordingly $S_\mathrm{circ}/\mathrm{I}_0 = (1\ 0\ 0\ \pm 1)'$. The reflection of polarized light off metallic mirrors with complex reflective coefficients $\tilde{r}_\mathrm{Pp/Ps} = r_\mathrm{Pp/Ps}\exp(i\delta_\mathrm{Pp/Ps})$ can be described by the Müller matrix M_Pol[12,29]

$$M_\mathrm{Pol}(\Psi_\mathrm{Pol}, \Delta_\mathrm{Pol}) = \frac{1}{2}\left(r_\mathrm{Pp}^2 + r_\mathrm{Ps}^2\right) \begin{pmatrix} 1 & -\cos(2\Psi_\mathrm{Pol}) & 0 & 0 \\ -\cos(2\Psi_\mathrm{Pol}) & 1 & 0 & 0 \\ 0 & 0 & \sin(2\Psi_\mathrm{Pol})\cos(\Delta_\mathrm{Pol}) & \sin(2\Psi_\mathrm{Pol})\sin(\Delta_\mathrm{Pol}) \\ 0 & 0 & -\sin(2\Psi_\mathrm{Pol})\sin(\Delta_\mathrm{Pol}) & \sin(2\Psi_\mathrm{Pol})\cos(\Delta_\mathrm{Pol}) \end{pmatrix}, \tag{6}$$

where $\tan(\Psi_\mathrm{Pol}) = r_\mathrm{Pp}/r_\mathrm{Ps}$ and $\Delta_\mathrm{Pol} = \delta_\mathrm{Pp} - \delta_\mathrm{Ps}$ is the phase shift induced by the reflection of the absorbing metallic surface.

The Stokes vector after reflection by the polarizer is calculated according to

$$S = M_{\mathrm{Pol}}\left(\Psi_{\mathrm{Pol}}, \Delta_{\mathrm{Pol}}\right) S_{\mathrm{Pol}}. \tag{7}$$

The degree of linear polarization P_{L} and circular polarization P_{C} is simply given by

$$P_{\mathrm{L}} = \frac{\sqrt{S_1^2 + S_2^2}}{S_0} \tag{8}$$

and

$$P_{\mathrm{C}} = \frac{S_3}{S_0} = \frac{\sin(2\Psi_{\mathrm{Pol}})\sin(\Delta_{\mathrm{Pol}})\sin 2\alpha}{1 - \cos(2\Psi_{\mathrm{Pol}})\cos 2\alpha}. \tag{9}$$

To yield perfectly circularly polarized light $P_{\mathrm{C}} = \pm 1$ requiring to fulfill the relations $\Delta_{\mathrm{Pol}} = \pm\pi/2$ and $\alpha = \Psi_{\mathrm{Pol}}$.

The above formalism is now used to determine for which material and geometry a reflection-based polarizer yields an optimal performance. To this end, we calculate the complex reflective coefficients $\tilde{r}_{\mathrm{Pp/Ps}}$ with the Darwin matrix formalism for different metallic mirror coatings both as a function of all grazing incident angles, θ, and within a photon energy range between 35 eV and 90 eV. We use tabulated values for the respective complex index of refraction.[30] For every metallic mirror coating and XUV photon energy, both the parameter α, controlling the ratio between s and p components of $\boldsymbol{E}$, and the parameter θ determine P_{C} and the reflectivity R. While larger grazing incident angles lead to a larger phase shift, Δ_{Pol}, and therefore to an increasing degree of circular polarization, the reflectivity decreases. We therefore define the figure of merit as RP_{C}^2 [31] and use an optimization algorithm to maximize it by varying the incident angle, θ, and rotation angle α. The best performance yields molybdenum with a protective cap layer (B_4C(2 nm)/Mo(25 nm)) in a four-mirror geometry (cf., Figure 2).

The results are summarized in Figure 1: it shows the figure of merit, $RP^2_{\mathrm{C},\theta,\alpha}$, where both parameters α and θ have been varied in the optimization calculation (dashed line). In comparison, we plot the figure of merit $RP^2_{\mathrm{C},\theta=12°,\alpha}$ for a constant grazing angle of incidence, $\theta = 12°$ and a variable rotation angle α (Figure 1(b)) as well as the corresponding degree of circular polarization $P_{\mathrm{C},\theta=12,\alpha}$ and the total reflectivity $R_{\theta=12,\alpha}$. Importantly, restricting the mirror setup to a fixed angle of incidence only results in a moderate loss of performance, while allowing a significant simplification of the device both with regards to its design as well as for alignment in tightly scheduled user operation. The degree of circular polarization is above 80% for M edge resonances of Fe, Co, and 75% for Ni, before it drops to approximately 50% at 90 eV. The increasing reflectivity as a function of photon energy is caused by absorption resonances of Mo below 40 eV and leads to an almost constant figure of merit of approximately 0.2 up to photon energies of 90 eV. The third harmonic of the FEL radiation is already efficiently suppressed with a total reflectivity on the order of 10^{-5} at 180 eV. Also note that in the spectral range of interest, the widely used material Au performs considerably worse with an achievable degree of circular polarization of ~75% and ~12% transmission at the Co M-edge resonance.

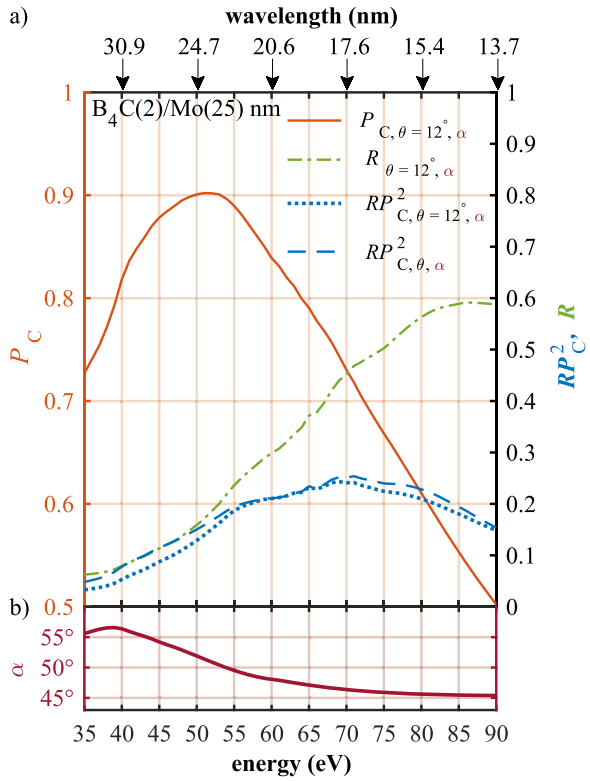

FIG. 1. Calculation for mirror coatings B_4C(2 nm)/Mo(25 nm): (a) Degree of circular polarization, P_{C} (red solid line), total reflectivity, R (green dashed-dotted line), and figure of merit, $RP_{\mathrm{C}}{}^2$, as a function of photon energy. The comparison between $RP_{\mathrm{C}}{}^2$ for a fixed angle of incidence $\theta = 12°$ (blue dotted line) and for a variable θ (blue dashed line) yields an almost negligible difference in performance. This allows a significant simplification of the design and effortless alignment for user operation. (b) Optimal angle of rotation, α, of the circular polarizer as a function of photon energy for a maximal figure of merit $RP^2_{\mathrm{C},\theta=12°,\alpha}$.

III. EXPERIMENTAL SETUP

The concept of the four-mirror reflection polarizer is shown in Figure 2(a). The initially linearly polarized FLASH1 pulses are reflected by four metallic mirrors and exit the device with an unaltered beam position and pointing but with a high degree of circular polarization. The three dimensional model is shown in Figure 2(b): the plane mirrors with dimensions (70 × 25 × 15 mm^3), longitudinal and sagittal slope errors of <1 arcsec, radius >10 km, and a surface roughness <0.5 nm (rms) are manufactured out of monocrystalline silicon (Pilz-Optics) and coated with a 25 nm thick molybdenum film protected by a 2 nm thick boron carbide layer (AXO Dresden GmbH). The four-mirrors are mounted on a monolithic holder with a fixed grazing angle of incidence $\theta = 12°$. The whole mirror assembly can be rotated around the beam axis ($-60° < \alpha < 60°$) by an infinite steel belt powered by an in-vacuum stepper motor (Phytron GmbH). Soft and hard end switches ensure safe operation and a reference angle for initialization of the device. The rotating part of the device is perfectly balanced such that no holding current is required to maintain a constant angle α. About 400 micro steps correspond to $\alpha = 1°$ rotation. Beam pointing deviations caused by small wobble errors of <30 μrad upon rotation are compensated by adjustments of mirror M_4

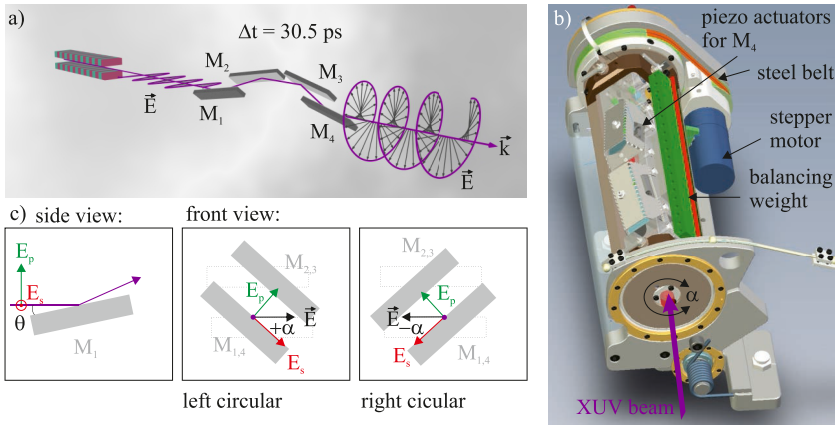

FIG. 2. (a) Artistic depiction of the four-mirror polarizer at FLASH1. (b) 3D model of the device: the mirror assembly can be rotated around the beam axis by angle $\boldsymbol{\alpha}$. The last mirror M_4 is adjustable by piezo actuators for compensation of small pointing deviations. (c) Front and side view of the four-mirror assembly. The grazing incident angle is fixed at $\theta = 12°$. The electric field vector of the incoming light pulses is decomposed into its s and p component and the rotation settings $\alpha = \pm 48°$ for negative and positive helicity are depicted. Adapted with permission from Höchst *et al.*, Surf. Sci. **352-354**(95), 998–1002 (1996). Copyright 1996 Elsevier.

via piezo actuators (Piezomechanik GmbH). With tabulated piezo settings, the device allows rapid switching (<10 s) of the XUV beam helicity without changing the beam position on the sample. The actuators may also be used to compensate small changes in the FEL beam position and pointing. The maximal displacement of the beam via the piezo actuators amounts to ±0.2 mrad and ±1 mrad in the horizontal and vertical directions, respectively (i.e., for $\alpha = 0$). A linear feedthrough allows to quickly and reproducibly move the assembly out and into the FEL beam. The device was designed in close collaboration with Steinmeyer Mechatronik Dresden GmbH, who also manufactured and assembled the device.

The four-mirror polarizer is placed in an ultra-high vacuum chamber, which has been built to fulfill the strict DESY vacuum guidelines regarding UHV compatible materials, manufacturing, assembly, content of hydrocarbons, and being particle free. This is particularly important to avoid any accumulative carbon contamination of the mirrors. The polarizer is positioned upstream of any focusing optics and can be used for any of the three BL beamlines at FLASH1 delivering the direct and "non-monochromatized" FEL beam.

For future time resolved pump-probe experiments with a synchronized optical laser, we determined the time delay of the FEL pulses occurring upon inserting the polarizer into the XUV beam (due to the additional path length of the geometrical configuration of the four-mirror assembly) to $\Delta t = 30.5$ ps.

IV. RESULTS

A. XUV-optical polarimeter

Before installation and commissioning at FLASH1, the performance of the four-mirror polarizer was characterized at the UE112 PGM-1 beamline of the BESSY II (HZB) synchrotron radiation facility.[32] For the polarization analysis, we used a Rabinovitch polarimeter,[7] consisting of a Mo-coated mirror placed under an incident angle of 40°. The angle is chosen to be close to the Brewster angle for photon energies between 45 eV and 68 eV and therefore provides a good contrast between the s and p component of the electric field vector. The reflected light is detected with a photodiode (Optodiodes, AXUV 100G). The mirror-detector assembly can be rotated by an angle β around the beam axis via a vacuum compatible rotation stage. The resulting Stokes vector for the light transmitted through the polarizer and analyzer is calculated via[11,12,17,29,33]

$$S_{\mathrm{AP}} = R^{-1}(\beta)\, M_{\mathrm{Ana}}(\Psi_{\mathrm{Ana}}, \Delta_{\mathrm{Ana}})\, R(\beta) \times R^{-1}(\alpha) M_{\mathrm{Pol}}(\Psi_{\mathrm{Pol}}, \Delta_{\mathrm{Pol}})\, R(\alpha)\, S. \quad (10)$$

The subscript "Ana" describes the respective parameters of the analyzer. The XUV diode detects the first component of the Stokes vector S_{AP0}. This is readily calculated and yields an expression which depends on Ψ_{Ana}, Ψ_{Pol}, and Δ_{Pol} as well as on the reflection amplitudes r_{Pp}, r_{Ps}, r_{Ap}, and r_{As}. The detector is a photodiode operated at normal incidence and is assumed to be insensitive to polarization, i.e., the detected signal is proportional to S_{AP0} which is independent of the phase shift Δ_{Ana} of the analyzer. The parameters can be retrieved by varying the two rotation angles α of the polarizer and β of the analyzer independently and fitting the measured data with expression S_{AP0}. The properties of the analyzer are deduced by repeating the measurements without the polarizer in the beam path yielding the corresponding first component of the Stokes vector S_{A0}.

We performed a set of measurements for 4 different photon energies, 47.2 eV, 52.7 eV, 59.9 eV, and 68.0 eV, corresponding to the respective $M_{2,3}$ resonances of Mn, Fe, Co, and Ni by varying the angle β for 21 different settings of α between −50° and 50°. Figure 3 shows two exemplary measurements and corresponding nonlinear least square fits according to expressions S_{A0} and S_{AP0} at a photon energy of 68 eV without (Figure 3(a)) and with the four-mirror polarizer set at an angle of $\alpha = 40°$ (Figure 3(b)). In Figure 3(c) we replot the calculated values for P_{C} and R together with

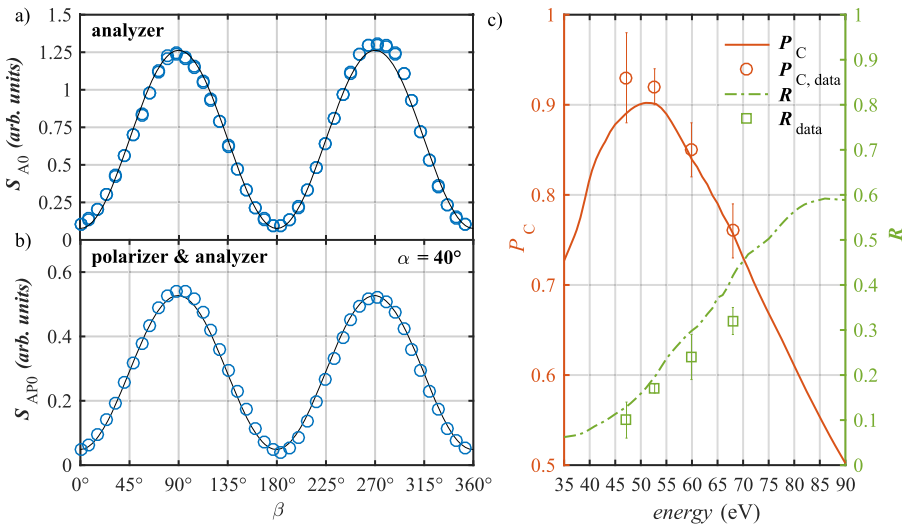

FIG. 3. Exemplary data sets (photon energy 68 eV) of β scans measured with the XUV polarimeter. The black lines are non-linear least square fits according to Equation (10). (a) Measured first component of the Stokes vector S_{A0} after transmission through the analyzer and (b) S_{AP0} after transmission through the four-mirror polarizer and the analyzer set at $\alpha = 40°$. The solid lines are nonlinear least square fits according to expressions S_{A0} and S_{AP0}. (c) Deduced degree of circular polarization, P_C (red open circles), and reflectivity, R (green open squares), in comparison with the optimization calculation (lines). We find a good agreement with P_C reaching up to 90% and R of several tens of percent.

the values retrieved from the polarimeter measurement. The error bars are calculated according to the standard deviation of the non-linear fits with the corresponding error propagation. We find a good agreement between calculations and measurements. We do note, however, that the reflectivity is slightly smaller than the calculated values, which may be related to imperfections in the mirror substrates or coatings. Importantly, the degree of circular polarization reaches 90% for Mn and Fe, approximately 85% for Co and more than 75% for Ni.

B. e-TOF polarimeter

To characterize the 4-mirror polarizer directly at the free-electron laser FLASH1, we have performed electron time-of-flight (e-TOF) polarimetry which is based on angle-resolved electron spectroscopy of rare-gas atoms. For a known atomic gas target with a specific ionized subshell,[34] the angular distribution of emitted photoelectrons sensitively depends on the linear polarization of the ionizing radiation and therefore allows to draw conclusions on the degree of circular polarization. The polarimeter consists of 16 independent e-TOF spectrometers mounted every 22.5° along a circle perpendicular to the FEL beam. The e-TOF polarimeter is designed for highly efficient polarization determinations and its functionality has been successfully confirmed at the Variable Polarization XUV Beamline P04 of PETRA III,[35] at the free-electron laser facility FERMI[27,36] and at LCLS at the SLAC National Accelerator Laboratory.[28,37] A dedicated data acquisition and analyzing system with 16 analog to digital converter (ADC) channels based on μTCA technology (sample rate of 4 GS s^{-1} and 12 bits resolution) allows to compare the measured angular electron distribution with the theoretical predictions to yield the degree and plane of the linear polarization on a single shot basis.

The photon energy of the FLASH1 pulses was set to 60 eV (20.66 nm) with a repetition rate of 10 Hz. We calibrated the transmission of each e-TOF detector by removing the four-mirror polarizer and using the linearly polarized FLASH1 pulses to measure the known angular distribution of Ne 2*p* photoelectrons. Subsequently, the polarizer was inserted into the FEL beam and the angular distribution of He 1*s* electrons was measured for varying rotation angles α. Here, linear polarized XUV radiation results in He 1*s* electrons emitted along the polarization axis, while for perfectly circularly polarized light, the electrons are emitted isotropically and all 16 detectors measure the same spectrum. For each setting of α, we accumulated a total of 2812 spectra, the analysis of the corresponding average spectra then results in the average degree of linear polarization P_{lin} as a function of α. We plot both the single shot data (shaded data points) and averaged values (filled circles with black edge) of P_{lin} in Fig. 4(a). As expected for the symmetric setting of $\alpha = 0°$, we measure almost perfectly linearly polarized light with $P_{lin} = 0.97$ whereas at the positions $\alpha = \pm 48°$, the degree of linear polarization is reduced to $P_{lin} = 0.52$. Under the assumption that the radiation is fully polarized, the degree of circular polarization, without distinction between left and right circular polarization, is calculated according to Equation (3), i.e.,

$$P_{circ} = \sqrt{1 - P_{lin}^2}. \tag{11}$$

The degree of circular polarization as a function of the rotation angle α is shown in Figure 4(a) and reaches a maximum of $P_{circ} = 0.85$ at $\alpha = \pm 48°$ which is in agreement with our calculated values (Fig. 1) and the polarimeter measurement (Fig. 3). The solid black line is the Stokes calculation according to Equation (7). Misalignment of α on the order of a few degrees has almost no influence on the resulting degree of circular polarization. The deviations between data and experiment for small α are due to the small, yet finite difference of the measured degree of linear polarization from 1, whereas the calculation assumes perfectly linear polarized radiation. This could be related to a small fraction of unpolarized light. The error bars for P_{circ} are calculated according to the error propagation of Equation (11) assuming a constant uncertainty of P_{lin} of 3%.[27] Note that as P_{lin} approaches 1, the error of P_{circ} diverges. In Figure 4(b) we show the single shot (shaded data points) and averaged recorded normalized intensity (filled circles with black edge) as a function of α. The observed relative decrease

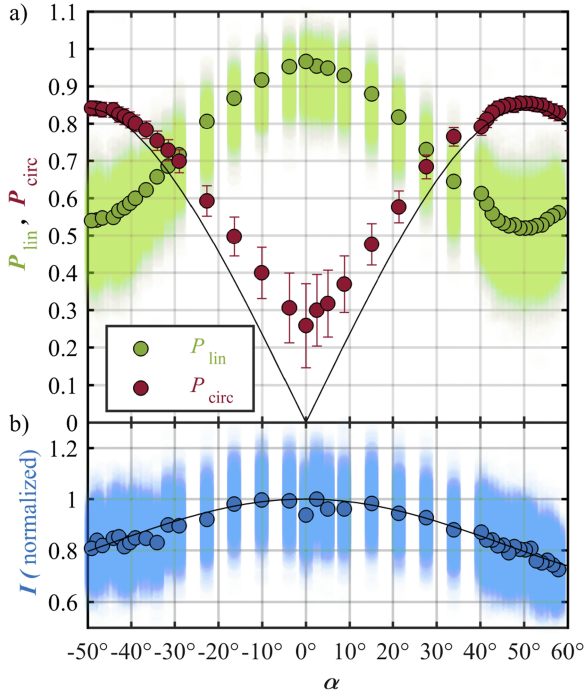

FIG. 4. (a) Measured degree of linear polarization P_{lin} and (b) reflected intensity I as a function of the rotation angle α. All single shot (shaded data points) and the corresponding average signals are shown (filled circles with black edge). The degree of circular polarization, P_{circ}, is calculated according to Equation (11) assuming a fully polarized incident FEL beam. The solid black lines are calculations according to Equation (7) and show a very good agreement. The error bars for P_{circ} are calculated according to the error propagation of Equation (11) assuming a constant uncertainty of P_{lin} of 3%. As P_{lin} approaches 1, the error of P_{circ} diverges.

of reflectivity to approximately 80% at $\alpha = \pm 48°$ is in excellent agreement with the theoretical predictions (black line) according to Equation (7).

C. Fourier transform holography of nanoscale magnetic domains

A resonant coherent imaging experiment of nanoscale magnetic domains, a few months after the successful commissioning, yielded another proof-of-principle of the four-mirror polarizer functionality. Ferromagnetic materials like Fe, Co, and Ni show a pronounced magnetic dichroic absorption at 3*p* core hole transitions in the XUV spectral range.[38] The difference in detected intensity between left and right circularly polarized light transmitted through the sample, $I_{\sigma^+} - I_{\sigma^-}$, is therefore directly proportional to the magnetization. Vice versa, magnetic circular dichroism presents direct and unambiguous evidence of circular polarization without having to assume anything about the contribution of unpolarized light.

The experiment was performed at the beamline BL2 of FLASH1 at DESY. The holography sample was manufactured for a standard transmission configuration:[39–41] A silicon nitride membrane (thickness 30 nm) supported by a silicon frame acts as a substrate. Via ion-beam lithography, we fabricated a circular object hole (diameter 2 μm) in a gold mask (thickness 250 nm) to define the field of view. Subsequently, the magnetic multilayer film Al(10)/Pt(2)/[Co(0.6)/Pt(0.8)]$_{20}$ /Al(3) nm was deposited via magnetron sputtering, and finally 5 reference holes with 60 nm and 80 nm diameter were added. The sample was placed 4 cm behind the focus of the FEL beam, resulting in a spot size of approximately 200 μm (FWHM). The coherently scattered XUV radiation was detected by an in-vacuum CCD camera placed 45 mm behind the sample. The direct beam was blocked by a beam stop. The intensity of the FEL pulses was attenuated by apertures and solid state filters to approximately 1.3 μJ to avoid the X-ray induced damage[26,42] and demagnetization. We emphasize that when determining the maximal acceptable FEL pulse intensity, it is important to take pulse to pulse fluctuations of the FEL into account as a single intense pulse may lead to a permanent reconfiguration of the magnetic domain pattern or may even destroy the sample. The pulse train repetition rate of FLASH1 is 10 Hz and we used 9 bunches spaced by 10 μs per pulse train, i.e., 90 pulses/s. We recorded one hologram for each helicity with an integration time of 60 s; the resulting magnetic difference hologram is shown in Figure 5(a). We observe pronounced magnetic speckle as well as strong reference-object fringe modulations (cf., inset of Fig. 5(a)) extending to a maximum momentum transfer of

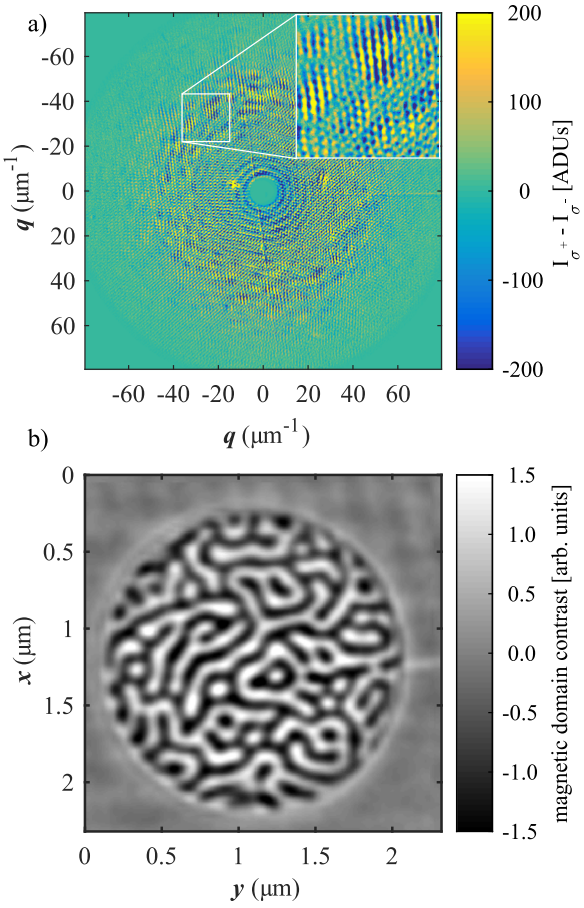

FIG. 5. (a) Difference hologram, $I_{\sigma^+} - I_{\sigma^-}$, showing pronounced magnetic speckle and strong object-reference modulations (cf., inset). The maximal momentum transfer amounts to 78 μm^{-1} corresponding to a minimal encoded spatial frequency of approximately 80 nm. (b) Reconstruction of the above hologram showing out-of-plane magnetic domains in opposite directions as black and white contrast. The magnetic domains with a size of approximately 70 nm are well resolved.

approximately $q = 78\,\mu\text{m}^{-1}$. This implies minimal encoded spatial frequencies of $2\pi/q \approx 80$ nm which in conjunction with the size of the reference holes determine the spatial resolution of the experiment. The real-space image is calculated via a two-dimensional Fourier transformation. For more detailed information on the experimental geometry and image reconstruction for FTH of magnetic nanostructures in the XUV spectral range, we refer the reader to a number of recent publications.[4,40,43,44]

We present the reconstructed real-space image of the nanoscale magnetic domains in Figure 5(b). The black and white regions within the 2 μm sized field of view correspond to out-of-plane magnetic domains pointing in opposite directions. The width of one magnetic domain is on the order of 70 nm and still well resolved. We can estimate the performance of the four-mirror polarizer by making a comparison with recently recorded FTH images of the identical sample at the free-electron laser facility FERMI which provides circularly polarized radiation with $P_C > 90\%$ with Apple-II-type undulators.[27] For the reconstruction of the magnetic domains shown in Figure 5(b), the photon density corresponded to 2×10^{10} photons/μm^2, approximately half the number reported in the experiment performed at FERMI of 4.8×10^{10} photons/μm^2.[44] Here the image was recorded slightly out of resonance (E = 61.4 eV) but showed a comparable absolute magnetic domain contrast and image quality. We can therefore conclude that the four-mirror polarizer fulfills its anticipated performance and enables users at FLASH1 for the first time to perform time resolved experiments with circular polarization, like for instance coherent imaging experiments of magnetic nanostructures.

V. CONCLUSION

In conclusion, we have presented a four-mirror reflection based polarizer for the free-electron laser facility FLASH1 operating in the XUV spectral range from 35 eV to 90 eV. Three independent measurements based on optical polarimetry, e-TOF spectroscopy, and magnetic circular dichroism give a consistent set of data demonstrating a high degree of circular polarization of up to 90% and a high total transmission of a few 10%. These values are in very good agreement with calculations. The monolithic design with fixed grazing incident angles allows a straightforward and fast alignment in tightly scheduled beamtimes with rapid and reproducible switching from left to right circular polarization. With the unique properties of FEL radiation, we envision new types of experiments in femto-magnetism ranging from magnetic circular dichroism spectroscopy to time-resolved coherent imaging of magnetic nanostructures. Enabling element specific spectroscopy of chiral light-matter interaction in (bio-)molecules makes this new device also attractive for a wider range of users from physics, chemistry, and life science.

ACKNOWLEDGMENTS

The support provided during installation and commissioning of the four-mirror polarizer by the scientists and technicians of the different divisions of DESY is appreciated. The Max-Born-Institute and TU Berlin group acknowledges financial support received by the BMBF Verbundforschung (Contract No. 05K10KTB) as well as from the Helmholtz Virtual Institute "Dynamic Pathways in Multidimensional Landscapes" (VH-VI-419). Support from the CNRS through the "PEPS SASELEX" and from the French ANR via the "UMAMI" project is acknowledged by the co-authors from Paris.

[1] N. Böwering, T. Lischke, B. Schmidtke, N. Müller, T. Khalil, and U. Heinzmann, "Asymmetry in photoelectron emission from chiral molecules induced by circularly polarized light," Phys. Rev. Lett. **86**(7), 1187–1190 (2001).

[2] F. Willems, C. T. L. Smeenk, N. Zhavoronkov, O. Kornilov, I. Radu, M. Schmidbauer, M. Hanke, C. von Korff Schmising, M. J. J. Vrakking, and S. Eisebitt, "Probing ultrafast spin dynamics with high-harmonic magnetic circular dichroism spectroscopy," Phys. Rev. B: Condens. Matter Mater. Phys. **92**(22), 1–5 (2015).

[3] B. Pfau, S. Schaffert, L. Müller, C. Gutt, A. Al-Shemmary, F. Büttner, R. Delaunay, S. Düsterer, S. Flewett, R. Frömter, J. Geilhufe, E. Guehrs, C. M. Günther, R. Hawaldar, M. Hille, N. Jaouen, A. Kobs, K. Li, J. Mohanty, H. Redlin, W. F. Schlotter, D. Stickler, R. Treusch, B. Vodungbo, M. Kläui, H. P. Oepen, J. Lüning, G. Grübel, and S. Eisebitt, "Ultrafast optical demagnetization manipulates nanoscale spin structure in domain walls," Nat. Commun. **3**, 1100 (2012).

[4] C. von Korff Schmising, B. Pfau, M. Schneider, C. M. Günther, M. Giovannella, J. Perron, B. Vodungbo, L. Müller, F. Capotondi, E. Pedersoli, N. Mahne, J. Lüning, and S. Eisebitt, "Imaging ultrafast demagnetization dynamics after a spatially localized optical excitation," Phys. Rev. Lett. **112**(21), 217203 (2014).

[5] M. Born and E. Wolf, *Principles of Optics* (University Press, Cambridge, 2011), p. 2015, ISSN: 00303992.

[6] R. N. Hamm, R. A. Macrae, and E. T. Arakawa, "Polarization studies in the vacuum ultraviolet," J. Opt. Soc. Am. **55**(11), 1460 (1965).

[7] K. Rabinovitch, L. R. Canfield, and R. P. Madden, "A method for measuring polarization in the vacuum ultraviolet," Appl. Opt. **4**(8), 1005 (1965).

[8] G. Rosenbaum, B. Feuerbacher, R. P. Godwin, and M. Skibowski, "Measurement of the polarization of extreme ultraviolet synchrotron radiation with a reflecting polarimeter," Appl. Opt. **7**(10), 1917 (1968).

[9] M. Schledermann and M. Skibowski, "Determination of the ellipticity of light and of optical constants by use of two reflection polarizers," Appl. Opt. **10**(2), 321 (1971).

[10] L. Nahon and C. Alcaraz, "SU5: A calibrated variable-polarization synchrotron radiation beam line in the vacuum-ultraviolet range," Appl. Opt. **43**(5), 1024–1037 (2004).

[11] A. Gaupp and M. Mast, "First experimental experience with a VUV polarimeter at BESSY," Rev. Sci. Instrum. **60**(7), 2213–2215 (1989).

[12] T. Koide, T. Shidara, M. Yuri, N. Kandaka, K. Yamaguchi, and H. Fukutani, "Elliptical-polarization analyses of synchrotron radiation in the 5-80-eV region with a reflection polarimeter," Nucl. Instrum. Methods Phys. Res., Sect. A **308**(3), 635–644 (1991).

[13] H. Höchst and F. Middleton, "To generate circular-polarized synchrotron radiation," Nucl. Instrum. Methods Phys. Res., Sect. A **347**, 107–114 (1994).

[14] K. Veyrinas, C. Elkharrat, S. Marggi Poullain, N. Saquet, D. Dowek, R. R. Lucchese, G. A. Garcia, and L. Nahon, "Complete determination of the state of elliptically polarized light by electron-ion vector correlations," Phys. Rev. A **88**(6), 1–5 (2013).

[15] M. Suzuki, K. Hanmura, T. Kotani, N. Yamaguchi, M. Kobayashi, and A. Misu, "Direct measurement of magnetic circular dichroism and Kerr rotation spectra in vacuum ultraviolet using four-mirror polarizer," Rev. Sci. Instrum. **66**(2), 1589–1591 (1995).

[16] H. Höchst, D. Zhao, and D. L. Huber, "$M_{2,3}$ magnetic circular dichroism (MCD) measurements of Fe, Co and Ni using a newly developed quadruple reflection phase shifter," Surf. Sci. **352-354**(95), 998–1002 (1996).

[17] B. Vodungbo, A. Barszczak Sardinha, J. Gautier, G. Lambert, C. Valentin, M. Lozano, G. Iaquaniello, F. Delmotte, S. Sebban, J. Lüning, and P. Zeitoun, "Polarization control of high order harmonics in the EUV photon energy range," Opt. Express **19**(5), 4346–4356 (2011).

[18]S. Long, W. Becker, and J. K. McIver, "Model calculations of polarization-dependent two-color high-harmonic generation," Phys. Rev. A **52**, 2262 (1995).
[19]H. Eichmann, A. Egbert, S. Nolte, C. Momma, B. Wellegehausen, W. Becker, S. Long, and J. K. McIver, "Polarization-dependent high-order two-color mixing," Phys. Rev. A **51**(5), R3414 (1995).
[20]A. Fleischer, O. Kfir, T. Diskin, P. Sidorenko, and O. Cohen, "Spin angular momentum and tunable polarization in high-harmonic generation," Nat. Photonics **8**(7), 543–549 (2014).
[21]O. Kfir, P. Grychtol, E. Turgut, R. Knut, D. Zusin, D. Popmintchev, T. Popmintchev, H. Nembach, J. M. Shaw, A. Fleischer, H. Kapteyn, M. Murnane, and O. Cohen, "Generation of bright circularly-polarized extreme ultraviolet high harmonics for magnetic circular dichroism spectroscopy," Nat. Photonics **9**, 99–105 (2014).
[22]G. Lambert, B. Vodungbo, J. Gautier, B. Mahieu, V. Malka, S. Sebban, P. Zeitoun, J. Luning, J. Perron, A. Andreev, S. Stremoukhov, F. Ardana-Lamas, A. Dax, C. P. Hauri, A. Sardinha, and M. Fajardo, "Towards enabling femtosecond helicity-dependent spectroscopy with high-harmonic sources," Nat. Commun. **6**, 6167 (2015).
[23]D. Wilson, D. Rudolf, C. Weier, R. Adam, G. Winkler, R. Frömter, S. Danylyuk, K. Bergmann, D. Grützmacher, C. M. Schneider, and L. Juschkin, "Generation of circularly polarized radiation from a compact plasma-based extreme ultraviolet light source for tabletop X-ray magnetic circular dichroism studies," Rev. Sci. Instrum. **85**(10), 103110 (2014).
[24]J. B. Kortright, S.-K. Kim, T. Warwick, and N. V. Smith, "Soft x-ray circular polarizer using magnetic circular dichroism at the Fe L_3 line," Appl. Phys. Lett. **71**(11), 1446, 1997.
[25]B. Pfau, C. M. Günther, R. Könnecke, E. Guehrs, O. Hellwig, W. F. Schlotter, and S. Eisebitt, "Magnetic imaging at linearly polarized x-ray sources," Opt. Express **18**(13), 13608–13615 (2010).
[26]T. Wang, D. Zhu, B. Wu, C. Graves, S. Schaffert, T. Rander, L. Müller, B. Vodungbo, C. Baumier, D. P. Bernstein, B. Bräuer, V. Cros, S. De Jong, R. Delaunay, A. Fognini, R. Kukreja, S. Lee, V. López-Flores, J. Mohanty, B. Pfau, H. Popescu, M. Sacchi, A. B. Sardinha, F. Sirotti, P. Zeitoun, M. Messerschmidt, J. J. Turner, W. F. Schlotter, O. Hellwig, R. Mattana, N. Jaouen, F. Fortuna, Y. Acremann, C. Gutt, H. A. Dürr, E. Beaurepaire, C. Boeglin, S. Eisebitt, G. Grübel, J. Lüning, J. Stöhr, and A. O. Scherz, "Femtosecond single-shot imaging of nanoscale ferromagnetic order in Co/Pd multilayers using resonant x-ray holography," Phys. Rev. Lett. **108**(26), 1–6 (2012).
[27]E. Allaria, B. Diviacco, C. Callegari, P. Finetti, B. Mahieu, J. Viefhaus, M. Zangrando, G. De Ninno, G. Lambert, E. Ferrari, J. Buck, M. Ilchen, B. Vodungbo, N. Mahne, C. Svetina, C. Spezzani, S. Di Mitri, G. Penco, M. Trovo, W. M. Fawley, P. R. Rebernik, D. Gauthier, C. Grazioli, M. Coreno, B. Ressel, A. Kivimäki, T. Mazza, L. Glaser, F. Scholz, J. Seltmann, P. Gessler, J. Grünert, A. De Fanis, M. Meyer, A. Knie, S. P. Moeller, L. Raimondi, F. Capotondi, E. Pedersoli, O. Plekan, M. B. Danailov, A. Demidovich, I. Nikolov, A. Abrami, J. Gautier, J. Lüning, P. Zeitoun, and L. Giannessi, "Control of the polarization of a vacuum-ultraviolet, high-gain, free-electron laser," Phys. Rev. X **4**(4), 1–15 (2014).
[28]A. A Lutman, J. P. MacArthur, M. Ilchen, A. O. Lindahl, J. Buck, R. N. Coffee, G. L. Dakovski, L. Dammann, Y. Ding, H. A. Dürr, L. Glaser, J. Grünert, G. Hartmann, N. Hartmann, D. Higley, K. Hirsch, Y. I. Levashov, A. Marinelli, T. Maxwell, A. Mitra, S. Moeller, T. Osipov, F. Peters, M. Planas, I. Shevchuk, W. F. Schlotter, F. Scholz, J. Seltmann, J. Viefhaus, P. Walter, Z. R. Wolf, Z. Huang, and H.-D. Nuhn, "Polarization control in an X-ray free-electron laser," Nat. Photonics **10**, 468 (2016).
[29]W. B. Westerveld, K. Becker, P. W. Zetner, J. J. Corr, and J. W. McConkey, "Production and measurement of circular polarization in the VUV," Appl. Opt. **24**(14), 2256 (1985).
[30]D. L. Windt, "XUV optical constants of single-crystal GaAs and sputtered C, Si, Cr_3C_2, Mo, and W," Appl. Opt. **30**(1), 15–25 (1991).
[31]B. A. Logan, R. T. Jones, and A. Ljubicic, "A figure of merit for gamma-ray polarimeters," Nucl. Instrum. Methods **108**, 603–604 (1973).
[32]G. Schiwietz, M. Beye, and T. Kachel, "UE112_ PGM-1 : An open-port low-energy beamline at the BESSY II undulator UE112," J. Large-Scale Res. Facil. **1**, A33 (2015).
[33]F. Schäfers, H.-C. Mertins, A. Gaupp, W. Gudat, M. Mertin, I. Packe, F. Schmolla, S. Di Fonzo, G. Soullié, W. Jark, R. Walker, X. Le Cann, R. Nyholm, and M. Eriksson, "Soft-x-ray polarimeter with multilayer Optics: Complete analysis of the polarization state of light," Appl. Opt. **38**(19), 4074 (1999).
[34]S. T. Manson and A. F. Starace, "Photoelectron angular distributions: Energy dependence for s subshells," Rev. Mod. Phys. **54**(2), 389–405 (1982).
[35]J. Viefhaus, F. Scholz, S. Deinert, L. Glaser, M. llchen, J. Seltmann, P. Walter, and F. Siewert, "The variable polarization XUV beamline P04 at PETRA III: Optics, mechanics and their performance," Nucl. Instrum. Methods Phys. Res., Sect. A **710**, 151–154 (2013).
[36]E. Ferrari, E. Allaria, J. Buck, G. De Ninno, B. Diviacco, D. Gauthier, L. Giannessi, L. Glaser, Z. Huang, M. Ilchen, G. Lambert, A. A. Lutman, B. Mahieu, G. Penco, C. Spezzani, and J. Viefhaus, "Single shot polarization characterization of XUV FEL pulses from crossed polarized undulators," Sci. Rep. **5**, 13531, 2015.
[37]G. Hartmann, A. O. Lindahl, A. Knie, N. Hartmann, A. A. Lutman, J. P. MacArthur, I. Shevchuk, J. Buck, A. Galler, J. M. Glownia, W. Helml, Z. Huang, N. M. Kabachnik, A. K. Kazansky, J. Liu, A. Marinelli, T. Mazza, H. D. Nuhn, P. Walter, J. Viefhaus, M. Meyer, S. Moeller, R. N. Coffee, and M. Ilchen, "Circular dichroism measurements at an x-ray free-electron laser with polarization control," Rev. Sci. Instrum. **87**(8), 083113 (2016).
[38]S. Valencia, A. Gaupp, W. Gudat, H.Ch. Mertins, P. M. Oppeneer, D. Abramsohn, and C. M. Schneider, "Faraday rotation spectra at shallow core levels: 3p edges of Fe, Co, and Ni," New J. Phys. **8**, 254 (2006).
[39]S. Eisebitt, J. Lüning, W. F. Schlotter, O. Hellwig, W. Eberhardt, and J. Stöhr, "Lensless imaging of magnetic nanostructures by X-ray spectroholography," Nature **432**, 885–888 (2004).
[40]S. Schaffert, B. Pfau, J. Geilhufe, C. M. Günther, M. Schneider, C. von Korff Schmising, and S. Eisebitt, "High-resolution magnetic-domain imaging by Fourier transform holography at 21 nm wavelength," New J. Phys. **15**, 093042 (2013).
[41]B. Pfau and S. Eisebitt, "X-Ray Holography," *Synchrotron Light Sources and Free-Electron Lasers* (Gabor, 2016), pp. 1–36, http://link.springer.com/referenceworkentry/10.1007/978-3-319-04507-8_28-1.
[42]C. Gutt, S. Streit-Nierobisch, L.-M. Stadler, B. Pfau, C. M. Günther, R. Könnecke, R. Frömter, A. Kobs, D. Stickler, H. P. Oepen, R. R. Fäustlin, R. Treusch, J. Feldhaus, E. Weckert, I. A. Vartanyants, M. Grunze, A. Rosenhahn, T. Wilhein, S. Eisebitt, and G. Grübel, "Single-pulse resonant magnetic scattering using a soft x-ray free-electron laser," Phys. Rev. B **81**(10), 2–5 (2010).
[43]C. M. Günther, E. Guehrs, M. Schneider, B. Pfau, J. Geilhufe, C. von Korff Schmising, S. Schaffert, and S. Eisebitt, "Experimental evaluations of signal-to-noise in spectro-holography via modified uniformly redundant arrays in the soft x-ray and extreme ultraviolet spectral regime," J. Opt. **19**(6), 064002 (2017).
[44]F. Willems, C. von Korff Schmising, D. Weder, C. M. Günther, M. Schneider, B. Pfau, S. Meise, E. Guehrs, J. Geilhufe, A. E. D. Merhe, E. Jal, B. Vodungbo, J. Lüning, B. Mahieu, F. Capotondi, E. Pedersoli, D. Gauthier, M. Manfredda, and S. Eisebitt, "Multi-color imaging of magnetic Co/Pt heterostructures," Struct. Dyn. **4**(1), 014301 (2017).